(will be inserted by hand later)

[CII] at 158 μm as a star formation tracer in late-type galaxies

A. Boselli[1], G. Gavazzi[2], J. Lequeux[3], and D. Pierini[4]

[1] Laboratoire d'Astrophysique de Marseille, BP 8, Traverse du Siphon, F-13376 Marseille Cedex 12, France
e-mail: Alessandro.Boselli@astrsp-mrs.fr
[2] Università degli Studi di Milano-Bicocca, Dipartimento di Fisica, Piazza dell'Ateneo Nuovo 1, 20126 Milano, Italy
e-mail: Giuseppe.Gavazzi@mib.infn.it
[3] DEMIRM and URA 336 du CNRS, Observatoire de Paris, 61 Av. de l'Observatoire, F-75014 Paris, France
e-mail: James.Lequeux@obspm.fr
[4] Ritter Astrophysical Research Center, The University of Toledo, 2801 West Bancroft, Toledo, OH 43606, USA
e-mail: pierini@ancona.astro.utoledo.edu

Abstract. We present a calibration of the massive star formation rate vs. [CII] luminosity relation based on a sample of nearby, late-type galaxies observed with ISO-LWS and imaged in the Hα+[NII] line. The relation holds for far-IR luminosities $10^8 \leq L_{FIR} \leq 10^{10.5} L_\odot$. The derived star formation rates have an uncertainty of about a factor of 10. Part of this uncertainty is due to the different mix of contributions to the [CII] emission from the different components of the interstellar medium in individual galaxies, as discussed in an appendix.

Key words. Galaxies: general – spiral – ISM – star formation – radio lines: galaxies

1. Introduction

Galaxies have transformed their primordial gas, mostly atomic hydrogen, into stars at a rate which can be variable with time. During merging with nearby companions, which were probably frequent in the high density environments of the early Universe, most of the gas might have been efficiently transformed into stars on short timescales ($\leq 10^8$ yr), forming elliptical galaxies. In spiral galaxies in the local Universe, the activity of star formation seems to be governed by the gas surface density, possibly modulated by galactic differential rotation (Kennicutt 1998a). The resulting star formation history of these objects should have been thus monotonic, governed by some of the physical properties of the original protogalaxy such as its angular momentum (Sandage 1986) or total mass (Boselli et al. 2001).

In order to understand the formation and evolution of galaxies, it is thus necessary to study the activity of star formation in objects of different types at different epochs. Quantifing the rate of star formation of normal, late-type galaxies in the local Universe is quite straightforward using Hα and UV data together with stellar population synthesis models (Kennicutt 1998a,b), once a correction for dust attenuation is made. This is not so easy for galaxies at higher redshift. Deep optical observations will provide UV rest-frame photometry, but the Hα line is shifted outside the optical domain for $z \geq 0.5$, while remaining in principle accessible in the near-IR up to $z \sim 6$. However the wide-field spectroscopic facilities suitable for statistical analysis which will be available in the near future, such as VIRMOS on the VLT, will be limited to $\lambda \leq 1.8$ μm, thus to $z \sim 1.7$.

Another problem is that a large fraction of galaxies are expected to form stars in violent starbursts at $z \geq 1$ (Steidel et al. 1999). The starburst regions are characterized by a high extinction, so that UV and Balmer lines cannot be reliably used: other indicators such as the far-IR luminosity should then be used (Kennicutt 1998a, b).

Given the low spatial resolution of available far-IR/submm data ($\sim$ 1 arcmin for IRAS and ISO at 100 μm, $\sim$ 15 arcsec for SCUBA), confusion is important at high redshifts. Mid-IR (MIR) surveys such as those performed with ISOCAM provide data with a higher spatial resolution ($\sim$ 6 arcsec), but the relation between MIR luminosity and star formation is still uncertain (Boselli et al. 1997a; 1998; Roussel et al. 2001).

Some far-IR forbidden lines, in particular the [CII] 158 μm one, are potentially better indicators of star formation in distant galaxies (Stacey et al. 1991a). The [CII] line is one of the main coolants of the interstellar gas. Heating of the interstellar gas is mainly due to photo–electrons emitted by dust grains and Polycyclic Aromatic Hydrocarbons (PAHs) submitted to ultraviolet radiation from stars (Bakes & Tielens 1994), both in

Send offprint requests to: Alessandro Boselli

the diffuse interstellar medium (ISM) (Wolfire et al. 1995) and in Photodissociation Regions (PDRs), at the interfaces between molecular clouds and HII regions (Tielens & Hollenbach 1985; Bakes & Tielens 1998). The photoelectric effect is due essentially to photons with $6 \leq h\nu < 13.6$ eV. In the field of a galaxy, this radiation is dominated by B3 to B0 stars with $5 \leq M \leq 20$ $M_\odot$ (e.g. Xu et al. 1994) but of course hotter, more massive stars can also contribute locally. However we cannot expect the intensity of the [CII] line from a galaxy to be simply proportional to the star formation rate (SFR) and to the intensity of the Hα line. This is due not only to the variety of [CII] line sources with their different physical conditions, which will be discussed further in the appendix, but also to the fact that the excitation of the upper fine-structure level of [CII] saturates at high temperatures and at high densities, as discussed e.g. by Kaufman et al. (1999; see their Fig. 2 and 3). Fortunately the [CII] line is only affected by extinction in extreme starbursts (Luhman et al. 1998; Helou 2000) or in edge-on galaxies (Heiles 1994), being not very optically thick ($\tau \approx 1$ in the Orion PDR: Stacey et al. 1991b, Boreiko & Betz 1996).

To summarize, the [CII] line cannot be a quantitatively accurate indicator of star formation in any galactic or extragalactic environment. However it is very strong, and next generation far-IR and submillimeter facilities such as FIRST-Herschel or ALMA will provide [CII] line intensities for large samples of galaxies at different redshifts (Stark 1997). In particular, the high angular resolution of ALMA will overcome the problem of confusion at high redshifts. It is thus useful to examine empirically to which extent the [CII] line can be used as a star formation indicator, and to calibrate it in terms of SFR in the local Universe using other tracers.

This is the aim of the present paper, which does not attempt to discuss in detail the physics of the emission in the [CII] line. We compare ISO-LWS [CII] to Hα data for a sample of 26 nearby galaxies (Sect. 2). Available complementary data are then used to empirically calibrate a relation between the [CII] luminosity and the SFR (Sect. 3). We emphasize that this calibration is limited to relatively quiescent galaxies. Sect. 4 contains a short dicussion and the conclusions. The relations between the far-IR emission of different components of the interstellar matter and their [CII] line emission are summarized in the Appendix.

2. The sample

An empirical calibration of the [CII] line as a star formation tracer can be obtained by comparing Hα and [CII] luminosities measured in the same aperture. For this reason we consider a sample of 18 Virgo galaxies observed with ISO-LWS.

The [CII] data are taken from Leech et al. (1999) and Smith & Madden (1997), while Hα+[NII] images are available from Boselli & Gavazzi (2002), Gavazzi et al. (2002) and Boselli et al. (2002). To increase the statistics, we add M82, which was imaged in the Hα+[NII] line by Boselli & Gavazzi (2002), NGC1569, whose Hα data are kindly made available to us by D. Bomans, and 6 objects (VCC 89, VCC 491 and VCC 1516, NGC 7469 and 7714, IC 4662) whose Hα data come from aperture photometry but whose optical disc, given their small angular size, has been covered to more than 40 % by the [CII] ISO-LWS beam. The final sample, which comprises the 26 galaxies listed in Table 1, is not complete in any sense.

Far-IR surveys at high redshifts will preferentially detect FIR-luminous galaxies, whose physical properties might significantly differ from those of the normal, late-type nearby galaxies analysed here. In our sample only two objects are luminous in the far-IR, M82 ($\log L_{FIR} = 10.51$ $L_\odot$) and NGC 7469 ($\log L_{FIR} = 11.37$ $L_\odot$), the latter being an active galaxy which should be considered with caution. We decided to add these two objects to test whether the present results can be extended to far-IR luminosities higher than $L_{FIR} \geq 10^{10.5}$ $L_\odot$.

The far-IR quiescent galaxies analysed here have $10^8 \leq L_{FIR} \leq 10^{10.5}$ $L_\odot$. Unless specified, all the results presented in this work are only valid for galaxies in this range of far-IR luminosity.

2.1. The data

The available data for the galaxies analyzed here are listed in Table 1, arranged as follow:

- Column 1: VCC denomination for the Virgo cluster galaxies (Binggeli et al. 1985), Messier, NGC or IC name for the other objects.
- Column 2: morphological type, from the VCC for Virgo galaxies, from NED for the other objects.
- Column 3: distance [Mpc], from Gavazzi et al. (1999) for Virgo, from the catalogue of Tully (1988) for the other galaxies, or from the redshift assuming $H_o = 75$ km s^{-1}Mpc^{-1}.
- Column 4: absolute B magnitude, as determined from our own photometry for the Virgo galaxies, from NED for the other objects.
- Column 5: H band luminosity, in solar units, defined as $\log L_H = 11.36 - 0.4 \times H_T + 2 \times \log(D)$, where H_T is the total H band magnitude and D the distance in Mpc. For the Virgo galaxies, total extrapolated near-IR magnitudes have been determined as described in Gavazzi et al. (2000) using the compilation of Boselli et al. (1997b; 2000) and Gavazzi et al. (1996a). K$'$ band magnitudes have been transformed into H magnitudes adopting a constant $H-K'$=0.25 (independent of type; see Gavazzi et al. 2000) when the colour index is not available. For the other galaxies H magnitudes are from 2MASS or from aperture photometry assuming an H band growth curve similar to the B band one.
- Column 6, 7 and 8: (Hα + [NII])$E.W.$ [Å], flux (- log, in erg cm^{-2}s^{-1}) extracted in the same circular apertures as LWS (i.e. 80 arcsec), and reference; the fluxes and equivalent widths from Kennicutt & Kent (1983) have been increased by 16 % as specified in Kennicutt

et al. (1994) (also Kennicutt, private communication); when the equivalent widths are not given, we estimate the underlying continuum from R band photometry using the relation: $R = 0.0$ mag $= 1.74 \times 10^{-9}$ erg cm^{-2}s^{-1}Å^{-1}.
– Column 9, 10 and 11: [CII] line flux, (- log, in erg cm^{-2}s^{-1}), equivalent width ([μm]) and reference. Fluxes and equivalent widths are all in the 80 arcsec circular apertures of LWS aboard ISO.
– Column 12: logarithm of the FIR luminosity, in solar units ($L_\odot = 3.83 \times 10^{26}$ W), $L_{FIR} = 4\pi D^2 \times 1.4 \times S_{FIR}$, where S_{FIR} is the far-IR flux in W m^{-2} between 42.5 and 122.5 μm, $S_{FIR} = 1.26 \times 10^{-14} \times (2.58 \times f_{60} + f_{100})$, where f_{60} and f_{100} are the IRAS fluxes at 60 and 100 μm respectively [Jy] (Helou et al. 1985). Far-IR data have been taken from different compilations for the Virgo galaxies (Thuan & Sauvage 1992; Soifer et al. 1989, Rush et al. 1993, and references therein), and from NED for the other galaxies.
– Column 13: comments on individual objects, from NED: 1= starburst, 2= LINER, 3= AGN.

The H band luminosity is a good tracer of the total dynamical mass of a galaxy (Gavazzi et al. 1996b): the mass to near-IR light ratio was found to be independent of mass for galaxies spanning the whole range in morphological type from Sa to Im and BCD. By normalizing the [CII] luminosity to the near-IR luminosity (within the same circular aperture) we remove the well known luminosity-luminosity or luminosity-mass scaling relations in a better way than by using optical luminosities.
However, since the aim of the present work is to establish a star formation tracer directely comparable to those which will be available for high-redshift galaxies from far-IR/submillimeter facilities, we will also use as a normalizer the continuum underlying the [CII] line. This leads to the determination of [CII] equivalent widths ([CII]$E.W.$, in μm). An advantage of using the continuum as a normalizer is that it is obtained in the same aperture of the [CII] line. A disadvantage is that this continuum is poorly determined, at least in the ISO-LWS observations (see Hunter et al. 2001).
Hα luminosities can be estimated from Hα+[NII] fluxes after correcting for contamination by the [NII] lines and for extinction. Given the good correlation observed between the [NII]/Hα ratios and L_H observed by Gavazzi et al. (in prep.), we use the statistical correction: log ([NII]/Hα) $= 0.35 \times \log L_H - 3.85$.
We use the same extinction correction as proposed by Boselli et al. (2001), namely A(Hα)=1.1 magnitudes for Sa$\leq$Scd and Pec galaxies, and A(Hα)=0.6 mag for the other objects, with the exception of M82 for which we take A(Hα)=3 mag (Gavazzi et al., 2002, in preparation).

3. Analysis

In the following we use the formalism of Boselli et al. (2001).

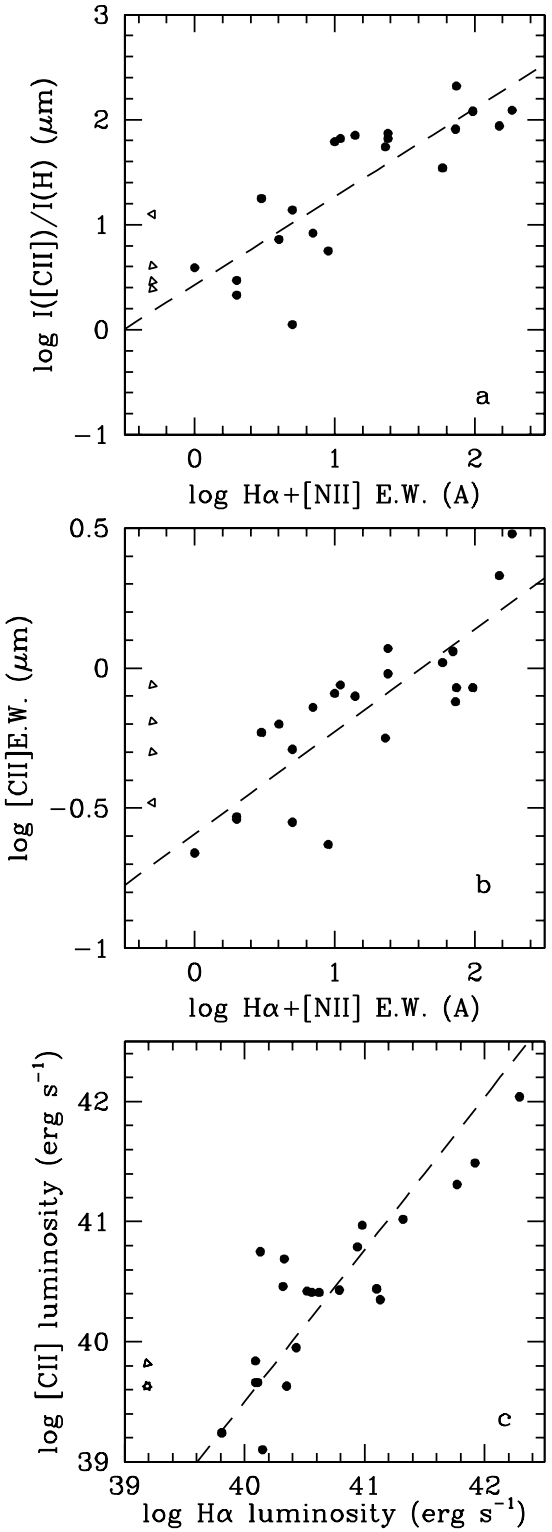

Fig. 1. The relationship between a) the [CII] line flux normalized to the H band flux and the (Hα + [NII])$E.W.$, b) the [CII] and the (Hα + [NII])$E.W.$ and c) the [CII] and Hα luminosities. The dashed lines give the best fit to the data (eq. 2 and Table 2) Open triangles are for [CII] and/or Hα undetected galaxies. We adopt arbitrary upper limits for the (Hα + [NII])$E.W.$ and for the Hα luminosity of 0.5 Å and 1.6 10^{39} erg s^{-1} respectively.

Table 1. The sample galaxies

Name	type	dist	M_B	L_H	(Hα + [NII])$E.W.$	f(Hα + [NII])	ref.	F([CII])	[CII]$E.W.$	ref.	L_{FIR}	comm.
		Mpc	mag	$L_\odot$	Å	erg cm^{-2} s^{-1}		erg cm^{-2} s^{-1}	μm		$L_\odot$	
(1)	(2)	(3)	(4)	(5)	(6)	(7)	(8)	(9)	(10)	(11)	(12)	(13)
$VCC66$	Sc	17	−19.93	10.22	24	12.20	1	12.11	1.16	1	9.31	
$VCC89$	Sc	32	−20.05	10.65	23^a	11.94^a	1	12.04	0.57	2	9.99	
$VCC92$	Sb	17	−21.28	11.03	5	12.33	2	12.06	0.51	1	9.82	3
$VCC460$	Sa	17	−19.98	10.84	9	12.33	6	12.57	0.23	1	9.52	2
$VCC465$	Sc	17	−19.46	9.88	73	11.71	3	12.08	0.76	2	9.29	
$VCC491$	Scd	17	−18.00	9.42	74	11.72	4	12.17	0.85	2	9.26	
$VCC857$	Sb	17	−19.24	10.53	1	12.64	2	12.85	0.22	1	8.99	2
$VCC873$	Sc	17	−19.41	10.39	11	12.44	5	11.76	0.87	1	9.68	
$VCC1003$	$S0a$	17	−20.57	11.04	5	12.11	2	12.85	0.28	1	9.08	2
$VCC1043$	Sb	17	−20.59	10.85	7	11.88	6	12.09	0.73	1	9.50	2
$VCC1110$	Sab	17	−20.46	10.96	2	12.56	6	12.68	0.30	1	9.28	2
$VCC1158$	Sa	17	−19.45	10.54	0	–	2	< 12.70	< 0.87	1	< 7.97	
$VCC1326$	Sa	17	−17.96	9.78	0	–	2	12.89	0.33	1	9.20	
$VCC1412$	Sa	17	−19.42	10.54	0	–	2	< 12.89	< 0.50	1	< 8.07	
$VCC1516$	Sbc	17	−19.01	9.85	10^a	12.29^a	6	12.09	0.81	2	9.06	
$VCC1690$	Sab	17	−21.47	11.07	3	12.31	2	11.82	0.59	1	9.90	3
$VCC1727$	Sab	17	−20.81	11.11	4	12.08	1	12.11	0.63	1	9.73	2
$VCC1813$	Sa	17	−19.77	10.84	0	–	2	< 12.70	< 0.65	1	8.58	
$VCC1972$	Sc	17	−19.27	10.50	14	11.79	4	11.72	0.79	1	9.65	
$VCC1987$	Sc	17	−20.32	10.66	24	11.73	4	11.55	0.96	1	10.04	
$VCC2070$	Sa	17	−20.01	10.76	2	12.34	4	12.89	0.29	1	8.72	3
$M82$	Pec	3.63	−18.94	10.69	70	10.35	2	9.86	1.15	4	10.51	1
$NGC1569$	IBm	1.6	−16.60	8.52	185	10.84	8	11.22	3.00	3	8.34	1
$NGC7469$	Sa	65.2	−21.43	11.18	97^a	11.50^a	7	11.64	0.86	5	11.37	3
$NGC7714$	Pec	36.9	−20.24	10.76	150^a	11.50^a	7	11.70	2.14	5	10.44	2
$IC4662$	Im	3	−16.10	8.78	59^a	11.04^a	1	11.90	1.04	3	8.18	

a: total values (galaxies whose optical sizes are comparable with the ISO-LWS beam).
References of Hα+[NII] data: 1: Kennicutt& Kent (1983); 2: Boselli & Gavazzi (2002); 3: Gavazzi et al. (2002); 4: Romanishin (1990); 5: Boselli et al. (2002); 6: Young et al. (1996); 7: Kennicutt et al. (1987); 8: Bomans, private communication; for references 1, 4 and 5 the fluxes and E.W.s are calculated in a 80 arcsec diameter aperture form the Hα+[NII] images from Boselli & Gavazzi (2002), Gavazzi et al. (2002) and Boselli et al. (2002).
References of the [CII] line data: 1: Leech et al. (1999); 2: Smith & Madden (1996); 3: Hunter et al. (2001); 4: Colbert et al. (1999); 5 Negishi et al. (2001), combined with Onaka, private communication.

The Hα luminosity gives a direct measure of the global photoionization rate of the interstellar medium due to high mass ($m > 10$ M$_\odot$), young ($\leq 10^7$ years) O-B stars (Kennicutt 1983; 1998a; Kennicutt et al. 1994). The total SFR can be determined by extrapolating the high-mass SFR to lower mass stars using an initial mass function (IMF) with a given slope α and upper and lower mass cutoffs M_{up} and M_{low} respectively. Assuming that $L_{\rm H\alpha}$ is proportional to the SFR, then we have:

$$SFR_{\rm H\alpha}({\rm M_\odot yr^{-1}}) = K_{\rm H\alpha}(\alpha, M_{up}, M_{low}) \times L_{\rm H\alpha} \qquad (1)$$

where $K_{\rm H\alpha}(\alpha, M_{up}, M_{low})$ is a proportionality constant between the Hα luminosity $L_{\rm H\alpha}$ (in erg s^{-1}) and the $SFR_{\rm H\alpha}$ (in M$_\odot$ yr^{-1}). The value of $K_{\rm H\alpha}(\alpha, M_{up}, M_{low})$, as a function of the slope α and of the upper and lower mass cutoffs M_{up} and M_{low} of the IMF, can be determined from stellar population synthesis models.

We plot the relationship between the [CII] line flux normalized to the H band (Fig. 1a) or the [CII]$E.W.$ (Fig. 1b), and the (Hα + [NII])$E.W.$. Normalized entities are used here to remove the first order dependence on luminosity; H magnitudes used in the normalization and Hα + [NII] parameters are determined within apertures comparable to the beam of the [CII] observations. H magnitudes ($Hmag$) are transformed into fluxes using the relationship: $I(H) = 1.03 \times 10^6 \times 10^{-Hmag/2.5}$ (mJy) (the resulting ratio $I([CII])/I(H)$ plotted in Fig. 1 is in units of μm).

Both figures show a strong correlation between the normalized [CII] line and the (Hα + [NII])$E.W.$ The relationship is shared by quiescent galaxies as well as by far-IR luminous objects, and is valid in the range $0 \leq$ (Hα + [NII])$E.W. \leq 200$ Å, which encompasses the whole normal, late-type galaxies population in the local Universe. This result confrims the expectations of Pierini et al. (1999). Figure 1c shows the relationship between the luminosities in the [CII] and Hα lines, the latter being corrected for extinction and [NII] contamination as described in Sect. 2.1.

This correlation is dominated by the scaling effect (bigger galaxies have more of everything). The correlation observed for the normalized entities shown in Fig. 1a and b, however, confirm that the excitation of the [CII] line is physically associated with the process of star formation, or more directly with the number of ionizing photons. This justifies the use of the [CII] line as a tracer of star formation.The best fit to the data for normalized entities are given in Table 2.

Figure 1c can be used to obtain the SFR from the [CII] luminosity. The best fit to the data gives:

$$\log L_{\rm H\alpha} = 8.875(\pm 0.326) + 0.788(\pm 0.098) \times \log L_{[CII]} \quad (2)$$

as determined on the 22 detected objects with a R^2=0.76.

The dispersion in the relation is high at low luminosities. We also remark that 20 out of the 22 galaxies used to estimate this relation are quiescent in the far-IR, i.e. $\log L_{FIR} \leq 10.50$ L$_\odot$.

Inserting $K_{\rm H\alpha}(\alpha, M_{up}, M_{low})$ for different IMFs in eq. (1), [CII] luminosities can be used to derive SFRs in M$_\odot$ yr^{-1} using eq. (2). For a Salpeter IMF (α=2.35) in the mass range between 0.1 and 100 M$_\odot$, the population synthesis models of Kennicutt (1998b) give $K_{\rm H\alpha}(\alpha, M_{up}, M_{low}) = 1/1.26\ 10^{41}$ (M$_\odot$ yr^{-1}/erg s^{-1}), thus:

$$SFR = 5.952\ 10^{-33} \times 10^{0.788 \times \log L_{[CII]}} \qquad {\rm M_\odot yr^{-1}} \quad (3)$$

from eq.(2), where $L_{\rm [CII]}$ is in erg s^{-1}. Values of $K_{\rm H\alpha}(\alpha, M_{up}, M_{low})$ for different IMFs can be found in Boselli et al. (2001).

In order to characterize the properties of the selected sample, thus to understand how universal this calibration is, we study the relation between the [CII] line emission and two parameters representative of the general properties of the target galaxies, the H band luminosity (as a tracer of the total mass) and the morphological type (Fig. 2).

Figure 2 shows that massive, early type spirals have in general a lower normalized [CII] emission than late-type, low mass ones, in agreement with Leech et al. (1999). This behaviour is identical to that observed for the star formation rate in the nearby Universe, as discussed in Boselli et al. (2001): massive galaxies form less stars per unit mass than low-mass objects.

We do not observe any particular relationship between two pure far-IR indices which will be easily observable in deep, far-IR surveys of the Universe, the [CII] $E.W.$ and the FIR luminosity, apart for a weak trend suggesting that far-IR luminous galaxies might have a somewhat higher [CII]$E.W.$. We remind that the proposed calibration in SFR of the [CII] line luminosity is valid for galaxies spanning the range in far-IR luminosity $8.0 \leq \log L_{FIR} \leq 10.50$ L$_\odot$ and $0.2 \leq$ [CII]$E.W. \leq 3.0$ μm. It is thus difficult to predict whether the present calibration can be applied to galaxies with $\log L_{FIR} \geq 10.50$ L$_\odot$.

4. Discussion and conclusion

The analysis carried out in the previous section has shown that the [CII] line luminosity can be taken as a star formation indicator in normal, late-type galaxies. It is however clear that this result cannot be extended to far-IR ultraluminous galaxies (ULIRG), where the ratio of the [CII] line over the continuum is a factor of ~ 10 lower than in normal late-type galaxies (Luhman et al. 1998).

The dispersion in the $L_{\rm H\alpha}$ vs. $L_{\rm [CII]}$ relation is a factor of ~ 3 (1 σ). The uncertainty on the determination of the SFR of galaxies using relations 3 is however larger. As shown in Charlot & Longhetti (2001), the uncertainty on the determination of SFR from Hα data using stellar population synthesis models is already a factor of ~ 3 when the data are properly corrected for dust extinction and [NII] contamination. If we take into account all the possible sources of error in the present determination of the Hα luminosity, and the uncertainty that can be introduced by the large dispersion observed in Fig. 1c, we can imagine that the resulting uncertainty in the determination of the SFR from [CII] line measurement is as high as a factor of ~ 10 statistically.

While the calibration of the Hα line luminosity in terms of SFR is limited by the accuracy of photoionisation and stellar population synthesis codes, and by the assumption that the initial mass function (IMF) is universal, the uncertainty introduced by the empirical calibration between $L_{\rm [CII]}$ and $L_{\rm H\alpha}$ should be significantly reduced once larger samples of galaxies with [CII] line data and Hα imaging are available. Part of this uncertainty may be due to the different mix of the contributions from different sources of the [CII] line emission within an individual galaxy and among galaxies of different Hubble types. We discuss this aspect in the Appendix.

Acknowledgements. We want to thank T. Onaka for providing us with unpublished LWS continuum data for all galaxies listed in Negishi et al. (2001), and D. Bomans for providing us with Hα data of NGC 1569. A.B. thanks S. Madden and A. Contursi for interesting discussions. We also thanks the referee, Gordon Stacey, for his insight and suggestions. This research has made use of the NASA/IPAC Extragalactic Database (NED) which is operated by the Jet Propulsion Laboratory, California Institute of Technology, under contract with the National Aeronautics and Space Administration.

References

Bakes E., Tielens A., 1994, ApJ 427, 822
Bakes E., Tielens A., 1998, ApJ 499, 258
Bennett C.L., Fixsen D.J., Hinshaw G., et al., 1994, ApJ 434, 587
Binggeli B., Sandage A., Tammann G., 1985, AJ 90, 1681 (VCC)
Boreiko R.T., Betz A.L. 1996, ApJ 467, L113
Boselli A., Gavazzi G., 2002, submitted to A&A
Boselli A., Lequeux J., Contursi A., et al., 1997a, A&A 324, L13

Table 2. Best fit to the relations between [CII] normalized entities and the Hα+[NII] E.W. (Å) (in logarithmic scales).

Variable	slope	constant	n. of objects	R^{2a}
$[CII]E.W.(\mu m)$	0.365 ± 0.056	-0.592 ± 0.169	22	0.68
$I([CII])/I(H)(\mu m)$	0.840 ± 0.134	0.427 ± 0.310	21	0.67

a: regression coefficient

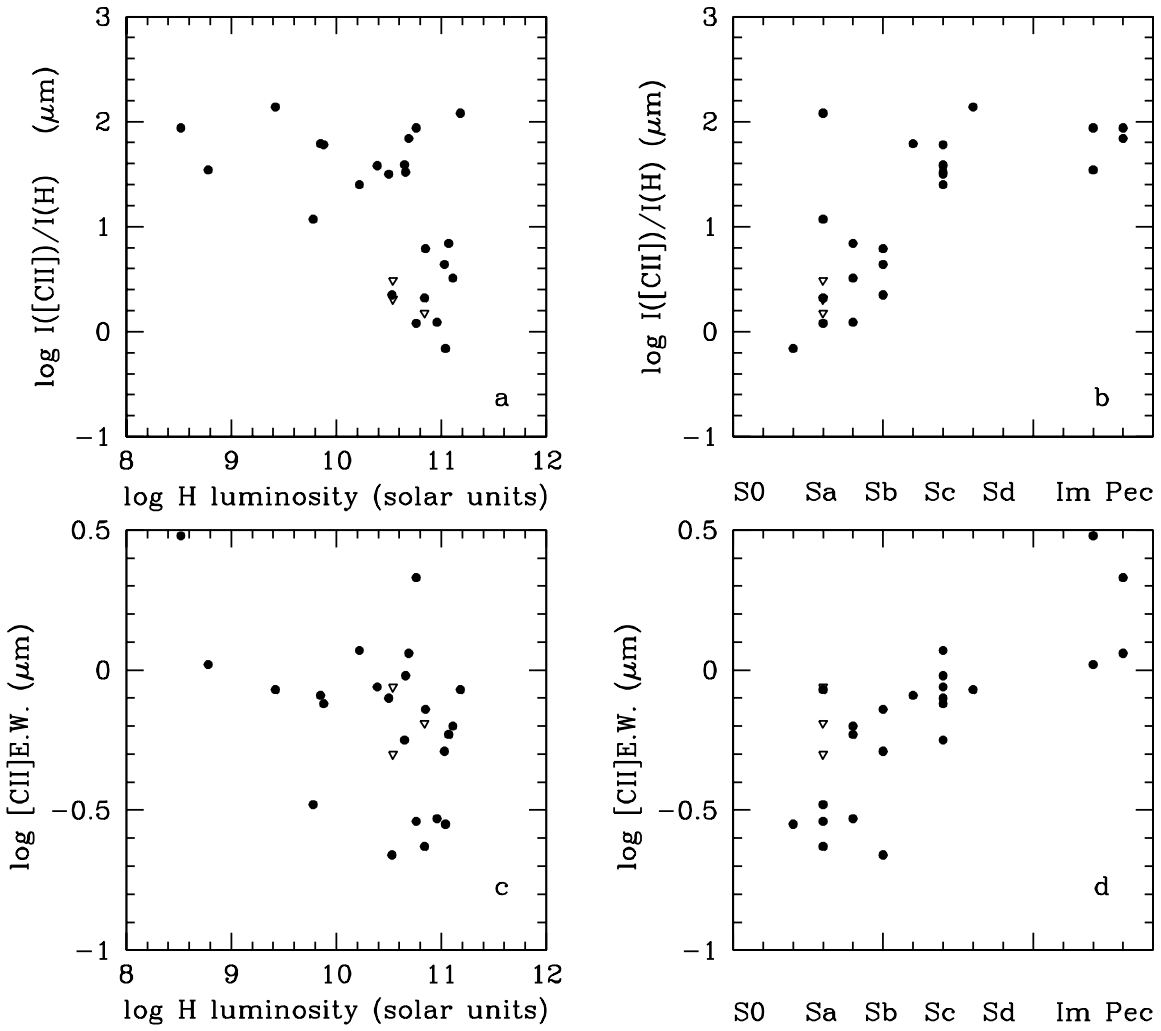

Fig. 2. The relationship between the [CII] line flux normalized to the H band flux and a) the H band luminosity, and b) the morphological type. The relationship between the [CII] *E.W.* and c) the H band luminosity, and d) the morphological type. Symbols as in Fig. 1.

Boselli A., Tuffs R., Gavazzi G., Hippelein H., Pierini D., 1997b, A&A 121, 507

Boselli A., Lequeux J., Sauvage M., 1998, et al. A&A 335, 53

Boselli A., Gavazzi G., Franzetti P., Pierini D., Scodeggio M., 2000, A&AS 142, 73

Boselli A., Gavazzi G., Donas J., Scodeggio M., 2001, AJ 121, 753

Boselli A., Iglesias-Paramo J., Vilchez J.M., Gavazzi G., 2002, submitted to A&A

Boulanger F., Cox. P., Jones A.P., 2000, in "Infrared Space Astronomy, Today and Tomorrow", Les Houches, ed. F. Casoli, J. Lequeux and F. David, Springer-Verlag, p. 253 to A&A

Charlot S., Longhetti M., 2001, MNRAS 323, 887

Colbert J., Malkan M., Clegg P., et al., 1999, ApJ 511, 721

Dale D.A., Helou G., Contursi A., Silbermann N., Kolhatkar S., 2001, ApJ 549, 215

Falgarone E., Puget J.L., 1985, A&A 142, 157

Gavazzi G., Pierini, D., Baffa C., et al., 1996a, A&AS 120, 521

Gavazzi G., Pierini, D., Boselli A., 1996b, A&A 312, 397
Gavazzi G., Boselli A., Scodeggio M., Pierini D., Belsole E., 1999, MNRAS 304, 595
Gavazzi G., Franzetti P., Scodeggio M., Boselli A., Pierini D., 2000, A&A 361, 863
Gavazzi G., Boselli A., Pedotti P., Gallazzi A., Carrasco L., 2002, submitted to A&A
Habart E., Verstraete L., Boulanger F., et al., 2001, A&A 373, 702
Heiles C., 1994, ApJ 436, 720
Helou G., Soifer B., Rowan-Robinson M., 1985, ApJ 298, L7
Helou G., 2000, in "Infrared Space Astronomy, Today and Tomorrow", Les Houches, ed. F. Casoli, J. Lequeux and F. David, Springer-Verlag, p. 337
Hunter D., Kaufman M., Hollenbach D., et al., 2001 ApJ 553, 121
Israel F.P., Maloney P.R., Geis N., Herrmann F., Madden S.C., Poglitsch A., Stacey G.J., 1996, ApJ 465, 738
Kaufman M., Wolfire M., Hollenbach D., Luhman M., 1999 ApJ 527, 795
Kennicutt R., 1983, ApJ 272, 54
Kennicutt R., 1998a, ARA&A 36, 189
Kennicutt R., 1998b, ApJ 498, 541
Kennicutt R., Kent S., 1983, AJ 88, 1094
Kennicutt R., Roettiger K., Keel W., van der Hulst J., Hummel E., 1987, AJ 93, 1011
Kennicutt R., Tamblyn P., Congdon C., 1994, ApJ 435, 22
Lagache G., Haffner L.M., Reynolds R.J., Tufte S.L. 2000, A&A 354, 247
Leech K., Völk H., Heinrichsen I., et al., 1999, MNRAS 310, 317
Li A., Draine B.T., 2001, ApJ 554, 778
Lockman F.J., Hobbs L.M., Shull J.M., 1986, ApJ 301, 380
Luhman M., Satyapal S., Fischer J., et al., 1998, ApJ 504, L11
Malhotra S., Kaufman M., Hollenbach D., et al., 2001, ApJ 561, 766
Mochizuki K., Nakagawa T., Doi Y., et al., 1994, ApJ 430, L37
Negishi T., Onaka T., Chan K., Roellig T., 2001, A&A 375, 566
Pak S., Jaffe D.T., van Dishoeck E.F., Johansson L.E., Booth R.S., 1998, ApJ 498, 735
Pierini D., Leech K., Tuffs R., Völk H., 1999, MNRAS 303, L29
Pierini D., Lequeux J., Boselli A., Leech K., Völk H., 2001, A&A 373, 827
Reynolds R.J., 1992, ApJ 392, L35
Romanishin W., 1990, AJ 100, 373
Roussel H., Sauvage M., Vigroux L., Bosma A., 2001, A&A 372, 427
Rush B., Malkan M., Spinoglio L., 1993, ApJS 89, 1
Sandage A., 1986, A&A 161, 89
Schmidtobreick L., Haas M., Lemke D., 2000, A&A 363, 917
Schwering P., 1989, A&AS, 79, 105
Smith B., Madden S., 1997, AJ 114, 138
Soifer B., Boehmer L., Neugebauer G., Sanders D., 1989, AJ 98, 766
Stacey G.J., Geis N., Genzel R., Lugten J.B., Poglitsch A., Sternberg A., Townes C.H., 1991a, ApJ 373, 423
Stacey G.J., Townes C.H., Poglitsch A., Madden S.C., Jackson J.M., Herrmann F., Gezel R., Geis N., 1991b ApJ 382, L37
Stacey G.J., Jaffe D.T., Geis N., Genzel R., Harris A.I., Poglitsch A., Stutzki J., Towne C.H., 1993, ApJ 404, 219
Stark A., 1997, ApJ 481, 587
Stasińska G., 1990 A&AS 83, 501
Steidel C., Adelberger K., Giavalisco M., Dickinson M., Pettini M., 1999, ApJ 519, 1
Thuan T., Sauvage M., 1992, A&AS 92, 749
Tielens A., Hollenbach D., 1985, ApJ 291, 722
Tully B., 1988, "Nearby Galaxies Catalogue", Cambridge University Press
Wolfire M., Hollenbach D., McKee C., Tielens A., Bakes E., 1995, ApJ 443, 152
Young J., Allen L., Kenney J., Lesser A., Rownd B., 1996, AJ 112, 1903
Xu C., Lisenfeld U., Völk H., Wunderlich E., 1994, A&A 282, 19

Appendix

In this Appendix we give a summary of our empirical knowledge of the relations between the [CII] line emission and the dust emission in the far-IR in various parts of the interstellar medium, and we discuss how the corresponding ratios compare with what is observed globally in galaxies. This subject is a rather complex one and the results are liable to changes when the data from ISO will be more fully analyzed. Thus this discussion is only provisional.

There are several possible sources for the interstellar far-IR forbidden lines, as discussed e.g. by Malhotra et al. (2001). Let us consider in particular the principal cooling lines of the neutral gas, [OI] 63μm and [CII] 158μm. While the [OI] line is nearly entirely emitted by dense photodissociation regions (PDRs), the [CII] line is emitted not only by these regions, but also by the diffuse neutral gas and by the ionized gas. The far-IR continuum emission at wavelengths larger than about 100 μm is due to big dust grains in thermal equilibrium, while at shorter wavelengths there is a contribution from smaller grains heated out of equilibrium by absorption of individual photons.

Let us now discuss briefly our knowledge of the [CII]/FIR ratios and, when available, of the [CII]$E.W.$, for different components of the interstellar medium. The results are summarized in Table 3.

A.1: Diffuse interstellar medium

Here the published observations concern essentially the local diffuse medium in the Solar neighbourhood, as observed at high galactic latitudes in particular by COBE. From the correlation of the [CII] line intensity $I([CII])$ with the column density of HI, Bennett et al. (1994) find a [CII] emission per H atom of the diffuse interstellar medium:

$$I_{\rm HI}([CII])/4\pi = (2.65 \pm 0.15)\, 10^{-26}\ {\rm erg\,s^{-1}\,H\,atom^{-1}}. \quad (4)$$

Together with a column density of HI of 3.3 10^{20} csc $|b|$ atom cm^{-2} (Lockman et al. 1986), this yields the following cosecant law for the intensity of the [CII] line emitted by the neutral diffuse medium:

$$I_{\rm HI}([CII]) = (6.96 \pm 0.39)\, 10^{-7}\ {\rm csc}\,|b|\ {\rm erg\,cm^{-2}\,s^{-1}\,sr^{-1}}. \quad (5)$$

From measurements of the Hα brightness at high galactic latitudes, Reynolds (1992) predicts an emission by the diffuse warm ionized medium (WIM) of:

$$I_{\rm WIM}([CII]) = 3.6\, 10^{-7}\ {\rm csc}\,|b|\ {\rm erg\,cm^{-2}\,s^{-1}\,sr^{-1}}, \quad (6)$$

in agreement with the upper limit $I_{\rm WIM}([CII]) < 6\, 10^{-7}$ erg cm^{-2} s^{-1} sr^{-1} given by Bennett et al. (1994) at the

galactic poles. Reynolds (1992) also predicts for the intensity $I([NII]_{205})$ of the [NII] 205μm line from the WIM:

$$I_{\rm WIM}([NII]_{205}) = 2.4\,10^{-8}\,{\rm csc}\,|b|\ {\rm erg\,cm^{-2}\,s^{-1}\,sr^{-1}}, \quad (7)$$

and a ratio between the intensities $I([NII]_{205})$ and $I([NII]_{122})$ of the [NII] 205μm and 122μm lines, respectively:

$$\frac{I_{\rm WIM}([NII]_{205})}{I_{\rm WIM}([NII]_{122})} = 1.4, \quad (8)$$

at the low-density limit. Bennett et al. (1994) observe $I([NII]_{205}) = (4 \pm 1)\,10^{-8}\,{\rm csc}\,|b|$ erg cm^{-2} s^{-1} sr^{-1} and $I([NII]_{205})/I([NII]_{122}) \approx 0.7$. The comparison with the predicted numbers, given the uncertainties on the gaseous abundances of N and C and on the observed intensities, leaves little doubt on the fact that the [NII] lines at high galactic latitudes come from the WIM, and that the predicted value of $I_{\rm WIM}([CII])$ is correct. The sum of $I_{\rm HI}([CII])$ and $I_{\rm WIM}([CII])$ is however smaller than the total observed intensity of the [CII] line, $I([CII]) = (1.43 \pm 0.12)\,10^{-6}\,{\rm csc}\,|b|$ erg cm^{-2} s^{-1} sr^{-1}, but the difference might not be significant given the uncertainties. To summarize, 2/3 of the [CII] line emission from the local diffuse medium comes from the neutral medium, and 1/3 comes from the warm ionized medium. Lagache et al. (2000) show that the FIR/submillimeter emissivity of dust associated with the two media is approximately the same, respectively $\tau/N({\rm HI}) = 8.3\,10^{-26}(\lambda/250\mu{\rm m})^{-2}$ and $\tau/N({\rm H^+}) = 1.1\,10^{-25}(\lambda/250\mu{\rm m})^{-2}$, with similar temperatures $T = 17.2$ K. The corresponding continuum brightness of the local diffuse medium at 158 μm is 4.94 csc$|b|$ MJy sr^{-1}, or 5.95 10^{-7} csc$|b|$ erg cm^{-2} s^{-1} μm^{-1} sr^{-1}. This allows one to calculate the equivalent width of the [CII] line from the local diffuse medium, as 1.8 μm if we use for the [CII] line intensity the observed contribution of the HI medium plus the estimated contribution of the WIM, or 2.4 μm if we use the line intensity observed directly by Bennett et al. (1994). The ratio of the [CII] line intensity to the far-IR intensity (defined as $I({\rm FIR}) = 1.26\ 10^{-14}[2.58\ I(60\mu{\rm m})/(1\ {\rm Jy/sr}) + I(100\mu{\rm m})/(1\ {\rm Jy/sr})]$ W m^{-2} sr^{-1}) is comprised between 0.034 and 0.045; we used for this determination the spectral energy distribution of the cirrus emission given by Fig. 3 of Boulanger et al. (2000).

We can simply estimate the variations of the [CII] line E.W. and of $I([{\rm CII}])/I({\rm FIR})$ with the the UV radiation field G_0 using the following simplifying assumptions: $I([{\rm CII}])$ is proportional to G_0 (in units of the Habing field, 1.6×10^{-3} erg cm^{-2}s^{-1}, $G_0 \approx 1$ near the Sun); the temperature of the big dust grains is $T_d = G_0^{1/6} \times 17.2$ K, and their emissivity is proportional to λ^{-2} (see above); the emission of the small dust grains giving an excess radiation at 60 μm is proportional to G_0, calibrated near the Sun using the cirrus spectral energy distribution of Fig. 3 of Boulanger et al. (2000). We find that $I([{\rm CII}])/I({\rm FIR})$ *decreases* with increasing G_0 in the range $1 < G_0 < 100$ (by a factor 2 at $G_0 = 10$ and a factor 3 at $G_0 = 100$), while [CII]*E.W. increases* by factors 1.8 and 5.4 respectively when G_0 increases from 1 to 10 and to 100. The reason why the line to continuum ratio gets smaller with increasing G_0, while the the equivalent width gets larger, is that the dust is getting warmer, shifting the far-IR continum to shorter wavelengths. More exact calculations can be made using the models of Li & Draine (2001) or of Dale et al. (2001), but the results are not expected to be substantially different.

No good observational information exists on the [CII]/FIR ratio in the diffuse medium of low-metallicity galaxies. However a comparison of the [CII] map of the Large Magellanic Cloud of Mochizuki et al. (1994) with the far-IR maps of Schwering (1989) suggests $I([{\rm CII}])/I({\rm FIR}) \simeq 0.010 \pm 0.005$ for the LMC.

A.2: Weak PDRs

Habart et al. (2001) give results from measurements with ISO on the PDR associated with the molecular cloud L 1721, illuminated by a B2 star, with $G_0 = 5$ - 10. The $I([{\rm CII}])/I({\rm FIR})$ ratio is of the order of 0.012 and the equivalent width of the [CII] line is about 6 μm. This is not very different from what we just predicted above for $G_0 = 10$ (respectively 0.02 and 4 μm). This small discrepancy may be understood if the density is lower than the critical density for the [CII] line.

The southern molecular cloud N 159S in the LMC is probably exposed to a similar far-IR intensity. Israel et al. (1996) give $I([{\rm CII}])/I({\rm FIR}) \geq 0.025$ for this cloud, somewhat higher than for L 1721. This is the highest value they quote for the LMC.

For the Orion giant molecular cloud at a one-degree scale, as described in Stacey et al. (1993) (their one-degree scan), the $I([{\rm CII}])/I({\rm FIR})$ ratio is of the order of 0.003, with $G_0 \sim 25$ (see their Sect. 4.2.3). This might be considered as typical for giant molecular clouds from which OB stars have recently formed.

A.3: Strong PDRs

Individual galactic strong and dense PDRs have values of $I([{\rm CII}])/I({\rm FIR})$ of the order of 5 10^{-4} (Stacey et al. 1991b). These very low values are a consequence of the saturation of the upper level of the 158 μm transition at high densities and radiation fields. An example is the $4' \times 4'$ "interface" region near the Orion nebula, as defined and discussed by Stacey et al. (1993). Strong PDRs in the Magellanic Clouds have considerably higher values of $I([{\rm CII}])/I({\rm FIR})$, of the order of 0.015 (Israel et al. 1996). As discussed by these authors, this exceptionally high value is associated with the low abundances of heavy elements in these galaxies. The effect of the low metal abundances is both direct (less far-IR emission from dust) and indirect (deeper penetration of UV light inside the PDRs) (see also Pak et al. 1998). However, due to the relatively poor linear resolution of the relevant observations, some contribution for an associated giant molecular cloud heated by a relatively weak UV radiation field might be included in the observing beam, raising the $I([{\rm CII}])/I({\rm FIR})$ ratio as discussed previously for the Orion region.

A.4: Quiescent molecular clouds

In a quiescent (i.e. with no or little star formation activity) molecular cloud, the [CII] line emission originates at the cloud surface while the far-IR emission comes also from the cloud interior. In our Galaxy, supposedly quiescent clouds are observed by Stacey et al. (1991b) to have $I([{\rm CII}])/I({\rm FIR}) \sim 1.1\ 10^{-3}$. They are not ordinary molecular clouds, however, but they are expected to be bounded by relatively strong PDRs because they are in fact immersed in a rather strong UV radiation field. Their higher $I([{\rm CII}])/I({\rm FIR})$ ratio compared to that of strong PDRs simply suggests that the upper level of the CII transition is less saturated, probably due to a combination of lower density and UV field. We have no information on the really quiescent molecular clouds, but it is clear that in some circumstances molecular clouds heated mainly by the visible and near-IR emission of relatively old stars can emit in the far-IR without any emission in the [CII] line. This may be the

case for molecular clouds in the bulge of M 31 (there is no direct evidence for the star formation suggested by Schmidtobreick et al. (2000) to be present inside some molecular clouds in this bulge). Similarly, regions of large molecular complexes heated by the far-IR radiation of the surrounding star-forming clouds (Falgarone & Puget 1985) are expected to emit in the far-IR but not in the [CII] line.

A.5: HII regions

Some fractions of the [CII] and far-IR global emissions may originate from within HII regions. However, these contributions are negligible with respect to those from other components of the ISM, on a galaxy scale. This conclusion is suggested by the comparison of the observed intensities of the [OIII], [NII], [CII] and [OI] lines with those predicted by photoionization models appropriate for HII regions, such as those of Stasińska (1990). It is then easy to see that the contribution of HII regions to the [CII], [NII] and [OI] lines is negligible at the scale of a galaxy. Similarly, the contribution of the dust inside the HII regions to the overall far-IR flux is negligible.

A.6: Comparison with galaxies

On average, the values of $I([\mathrm{CII}])/I(\mathrm{FIR})$ and $[\mathrm{CII}]E.W.$ observed for our galaxies are of the order of 3 10^{-3} and of 0.7 μm respectively, but the dispersion is large. These values are smaller than the corresponding values for the diffuse gas alone. For the irregular galaxies of Hunter et al. (2001), $I([\mathrm{CII}])/I(\mathrm{FIR})$ = 2 - 6 10^{-3}. For the LMC as a whole, $I([\mathrm{CII}])/I(\mathrm{FIR}) = 0.01$ (Israel et al. 1996). No conclusion can be reached on the respective contributions of the different interstellar components for the [CII] emission of the LMC, because the $I([\mathrm{CII}])/I(\mathrm{FIR})$ ratios are similar within the (large) errors for PDRs and for the diffuse matter (but see the discussion above on the strong PDRs in the Magellanic clouds). For spiral galaxies, it is clear that the contributions of the PDRs to the emission of the [CII] line should be added to those of the diffuse neutral and ionized media. However we have seen that in these galaxies the strong PDRs exhibit values of $I([\mathrm{CII}])/I(\mathrm{FIR})$ of about 5 10^{-4}. As a consequence, strong PDRs cannot be the only contributors to the [CII] and far-IR emissions in normal spiral galaxies: weak PDRs with $I([\mathrm{CII}])/I(\mathrm{FIR})$ of 0.003 to 0.015, and the diffuse medium with $I([\mathrm{CII}])/I(\mathrm{FIR}) \sim 0.04$, must also contribute to explain the average ratio of 0.003. It is however possible to account for the properties of galaxies by a simple one-component analysis using single values of the density and UV radiation field, as those of Hunter et al. (2001), Malhotra et al. (2001) and Negishi et al. (2001). In such a model, about 30,000 giant molecular clouds similar to the 1-degree Orion cloud of Stacey et al. (1993), each one with a [CII] line luminosity of 1.5 10^{-3} $L_\odot$, would explain the both the luminosity of the [CII] line and the $I([\mathrm{CII}])/I(\mathrm{FIR})$ ratio of our Galaxy. Such simple models might well be justified for active star-forming galaxies, in which dense PDRs dominate by far the emission of the [CII] line. In more normal galaxies, however, all the components we have described are likely to contribute to some extent and these simple models have to be considered with caution. In some galaxies, the contribution of low-density neutral gas to the [CII] line can reach as much as 50% of the total, as shown by Pierini et al. (2001). Unfortunately, it does not yet seem possible to disantangle the contributions of the various intestellar components to the emission of the [CII] line and of the FIR continuum.

Table 3. Characteristics of the [CII] emission different galactic and extragalactic environments.

Component	G_0	I([CII])/I(FIR)	$[CII]E.W.$ μm
Diffuse gas	1	0.04	2
	10	0.02	4
Diffuse gas in LMC	10	$\simeq 0.01$	–
Weak PDR	$3-10$	0.012	6
Weak PDR in LMC	10	> 0.02	–
Orion molec. complex	25	0.03	–
Strong PDR	10^3-10^5	5 10^{-4}	–
Strong PDR in LMC	10^3-10^5	0.02	–
Normal spiral galaxies	–	3 10^{-3}	0.7
Irregular galaxies	–	$2-6$ 10^{-3}	–
LMC	–	0.01	–

A multi-component analysis is probably not feasible at present due to the lack of analyzed data, but it might become possible in the near future considering not only the emission in the fine-structure lines and the dust infrared continuum, but also the emission in the CO lines. This does not prevent the use of the [CII] line as an indicator of star formation, but shows that for the moment this indicator can only be calibrated empirically as we are doing here.